APPLICATION OF ARTIFICIAL NEURAL NETWORK TECHNIQUES FOR MEASURING GRAIN SIZES DURING SUGAR CRYSTALLISATION

AUBREY Z MHLONGO and MICHAEL J ALPORT

Applied Physics Group, School of Pure and Applied Physics,
University of Natal, Durban 4041, South Africa
E-mail: mhlongo2@cyclops.und.ac.za / alport@nu.ac.za

Abstract

This paper discusses the development of a system for the automated real-time measurement of crystal size distributions during crystallisation. An optimised selection of the Daubechies wavelet coefficients is used as input to a Multi–Layer Perceptron artificial neural network to characterise the crystal scale lengths. This technique gives significant advantages over the sampling-based measurements, which require an individual measurement of single crystals. Test results obtained using simulated crystals, and actual images from a crystallisation pan and a laboratory crystaloscope are presented.

Keywords: Artificial neural network, wavelet, sugar crystallisation, image analysis, crystal sizing

Introduction

Since McCulloch and Pitts built the first simplified model of a neural network in 1943, using analog electrical circuits, the digital software implementation of different neural architectures has become widespread for the control and monitoring of industrial processes.

Usually, the inputs to a neural network are obtained from sensors that measure such parameters as pressure, temperature, pH and flow rate. However the inputs may also be obtained from images. For example, in industrial flotation process, since it has been shown that there is relationship between froth appearance and the concentration of precious and base metals in the pulp, it is possible to extract features of images from an online machine vision system and relate them to plant performance (Moolman *et al.,* 1996).

Sugar crystallisation is one of the significant stages in the sugar manufacturing process. The crystallisation is carried out in vacuum pans where the sugar is separated from the syrup in the form of homogeneous colourless crystals. This process involves first loading the pan with sub-saturated syrup and heating under vacuum until conditions of over saturation are reached. Then sugar powder is fed in to seed the crystals, which are grown. Currently, an operator controls crystal growth using a variety of indirect measurement techniques such as conductivity (Prasad and Singh, 1999), boiling point elevation, stirrer torque and radio frequency measurements in addition to visual inspection. There have been a number of image-based techniques to determine the size of the raw sugar crystals using different methods such as direct use of a microscope (Dalziel *et al.,* 1999), (Miller and Beath, 2000) or tomography (Jones *et al.,* 2000).

It has also recently been suggested (Palenzuela and Cruz, 1996), (Peacock, 1998), that neural networks (Principe *et al.,* 2000) can be used to control the crystallisation process by the direct observation of the crystals. Our approach involves some data reduction.

In this paper we explore the feasibility of obtaining the real-time mean crystal size from single images of crystals that are either splashed onto the viewing port window of a crystallisation pan or viewed directly through an immersed crystaloscope.

We have considered the problem in a three-stage process.

a. Image segmentation: We have investigated the use of cross-polarisers to improve the contrast between the crystals and their background.

b. Feature Extraction: Both Fast Fourier Transform and wavelet transforms have been used to reduce the dimensionality of the images. We find that the wavelet coefficients are more efficient inputs for the neural network.

c. Teaching a neural network: A Multi-Layer Perceptron (MLP) artificial neural network has been found to give a good prediction of the measured mean crystal diameter.

The effects of non-uniform illumination can complicate the analysis of the crystal images. Also, the variation of refractive effects due to the different angles presented by the various crystal faces cause some faces to appear very dark and others to be almost indistinguishable from the bright background. We first explored various polarization techniques to improve the image quality of the crystals and then investigated problems (b) and (c) by using one and two-dimensional simulated images of crystals. Finally, we then applied these results to >200 crystal images obtained from a pan crystalliser and a laboratory crystaloscope.

Method

Experimental Configuration

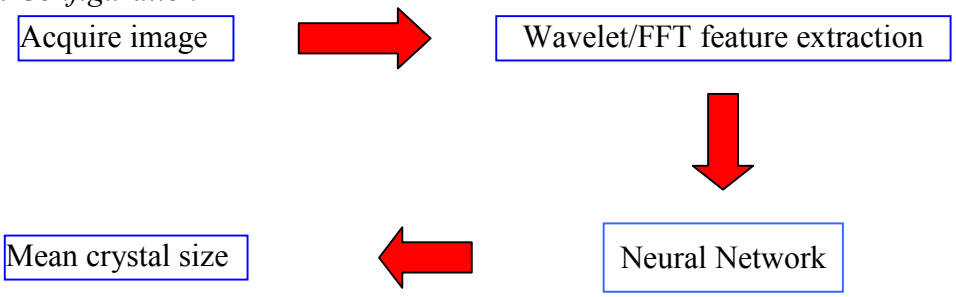

Figure 1: Procedure used to obtain a measurement of mean crystal size directly from images of the crystal.

The sequence of operations required to analyse the crystal images is shown diagrammatically in Figure 1, and the pan experimental configuration is shown in Figure 2. The crystal images were first acquired by a hi-resolution black and white CCD camera and then digitised by a PC frame grabber. In the first experimental configuration, the camera was focused on the back side of the glass port and imaged the crystal solution that was splashed onto the glass by the boiling process. In the second experimental configuration, images of the crystals were obtained from a reconditioned Crystaloscope immersed in a beaker containing a solution of glycerine and sugar crystals.

The wavelet coefficients were calculated using the IDL software package.[3] For both experimental setups, an optimized subset of the Daubechies wavelet coefficients (Daubechies,1992) were used as inputs to train a MLP neural network[4] The desired mean crystal size for each image was determined by manually placing a rectangle over the crystal using the mouse cursor. The average mean crystal size, D, was calculated from the length (L) and width (W) of these crystals by assuming that the third dimension (depth) was equal to the length as:

$$D = \sqrt[3]{WL^2} \qquad (1)$$

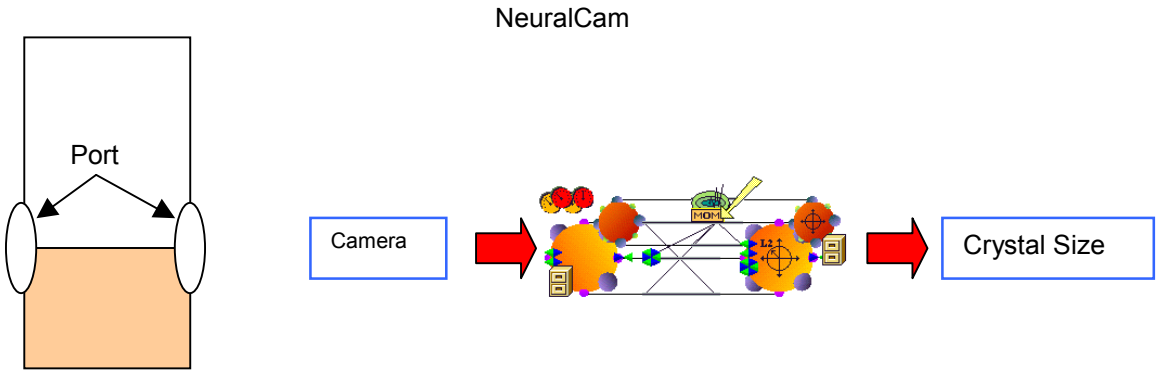

Figure 2: Schematic of the experimental configuration used to obtain crystal images from the Tongaat- Hulett crystallisation pan.

For the pan setup, as shown in Figure 2, the camera was mounted ~15cm in front of a port and during the period November 1999-July 2000, about 300 images were captured. The wavelet coefficients of these images were then subsequently used as inputs to the neural network, which, after training was able to predict the average crystal size in each image. Various illuminating geometries were used, including a circular fluorescent tube located outside the port at the back of the pan.

Image segmentation

A specific problem with the imaging setup was that the central region within the crystal boundary could be as bright as the surrounding background as seen in **Figure 3**(a). If only local pixel information is used, it is difficult to distinguish the crystal from its surroundings. By mounting crystals on a microscope slide and viewing them under an optical microscope it was found that using two crossed polarisers could minimize this problem. When the optically active crystals were placed between two crossed polarisers, the light that travels through the background is cut-off by the second filter. On the other hand, light passing through the crystal will be slightly rotated, and hence produces a bright feature as shown in Figure 3(b).

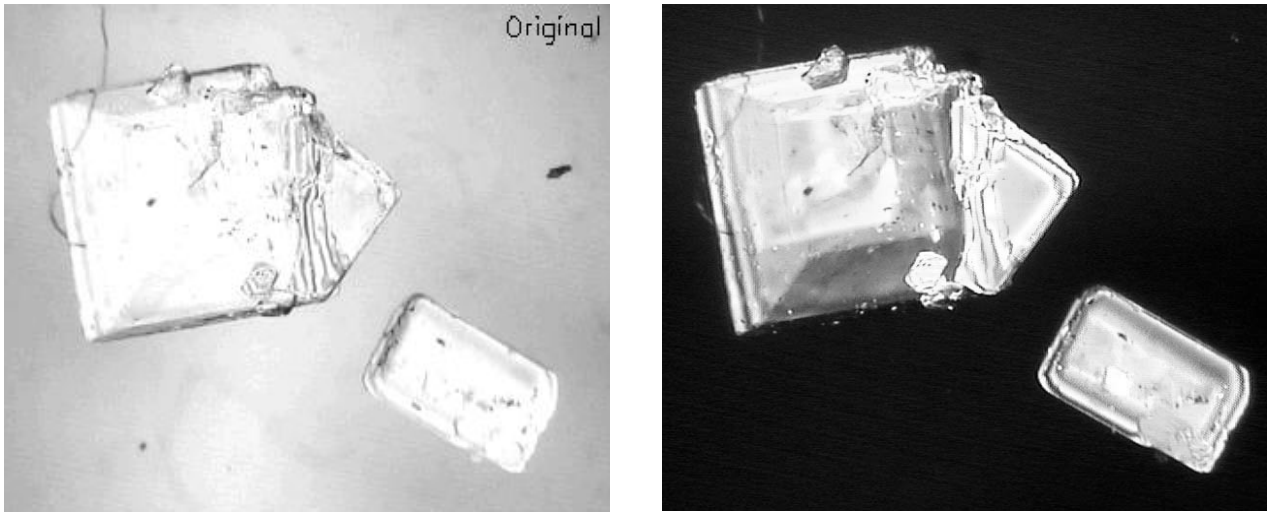

(a) (b)

Figure 3. (a) The original image of the crystal showing that the central region of the crystal can be as bright as the background. (b) The same image after it has been sandwiched between two crossed polarisers.

This technique was then repeated using the crystaloscope in the following way. In the crystaloscope, as shown in Figure 4, light from a lamp is reflected multiple times by mirrors in the crystaloscope column before passing through the sight gap, containing the massecuite. The camera thus images the backlit crystals. We investigated two different locations for the crossed polarisers, A-B and B-C (see Figure 4 below). With the polarisers located at B-C, i.e. with the massecuite sandwiched between the two polarisers, we should expect to duplicate the improved contrast obtained with the dry crystals.

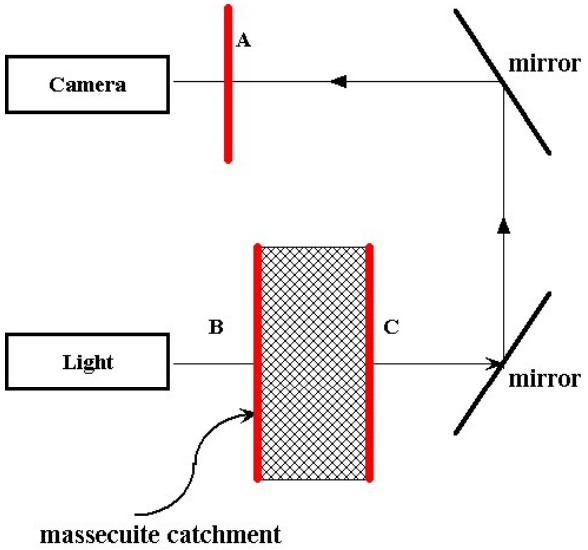

Figure 4: The crystaloscope light system showing the light path from the source through the massecuite to the camera.

To quantify the behaviour of the two-polariser configurations, for each configuration we calculated the contrast $C(\theta)$ defined by

$$C(\theta) = \frac{I_{in} - I_{out}}{I_{in} + I_{out}} \quad (2)$$

as a function of the angle, θ, between the polarisers. Here I_{in} is the average pixel intensity in a crystal, and I_{out} the average intensity outside the crystal. Ideally, we need to achieve as high a value of C as possible in order to discriminate between the crystal and the surroundings.

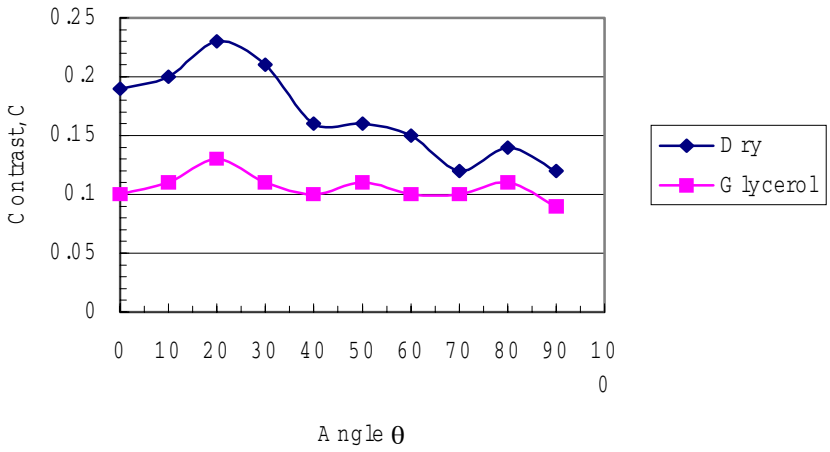

Figure 5: The change in contrast as a function of polariser angle.

Confirming our earlier light microscope measurements, Figure 5 shows that there is good contrast of C~0.24 at θ~20° when the dry crystals were placed between the polarisers. However, there is only slight improvement when the crystals are immersed in the glycerine. The reason for this is not quite clear but could be related to a depolarising effect due to enhanced multiple reflections in the crystaloscope. Similar measurements have not yet been duplicated with a massecuite solution.

Use of simulated crystals

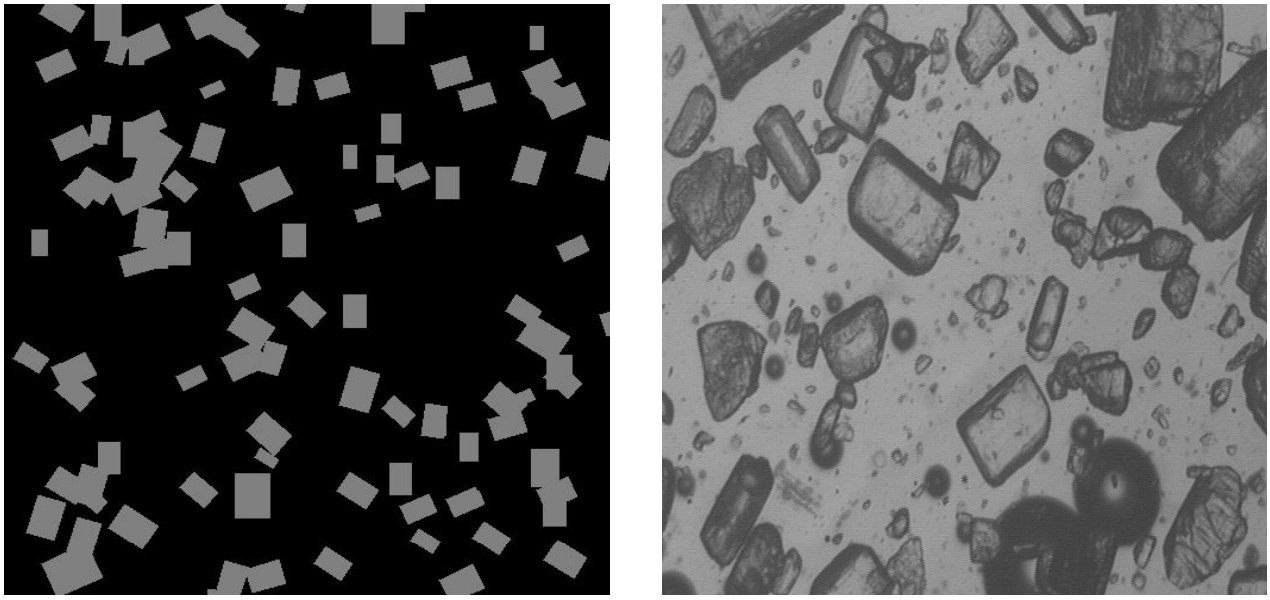

(a) (b)

Figure 6. (a) An example of a 2D artificial array of crystals with a 1:1 aspect ratio. Each image contained 50 crystals, randomly distributed about a pre-chosen mean crystal size. There is some overlap of crystals. (b) An image of the crystals obtained from the crystaloscope.

To investigate the performance of the imaging algorithms and the artificial neural network, images of simulated crystals consisting of grey rectangles of varying aspect ratio and orientation were generated and placed on a black background as shown in Figure 6(a). In this way, non-ideal aspects of real images, such as crystal orientation, overlapping, noise and non-uniform illumination, could be separately examined. The crystal dimensions (length and width) were chosen randomly from a Gaussian distribution having a chosen average width/length and standard deviation. The position and orientation of each crystal was chosen randomly from a uniform distribution. In addition, the position of the crystals could be chosen to overlap or not, as required.

Training the Artificial Neural Network

The artificial neural network must first be trained so as to minimise the mean squared error between the output of the neural network and the desired output. In general, the input data was divided into three sets: typically, 60% were used for training, 15% for cross-validation during training and the remaining 25% were reserved for testing. The MLP employed had four processing units in one hidden layer. Training was stopped after 200 epochs or cycles through the data set.

For the N real crystal images, the mean percentage error, $\mathcal{M}$, defined as

$$\mathcal{M}[\%] = \left(\frac{\sum_{i=1}^{N} \frac{|P_i - D_i|}{D_i}}{N} \right) \times 100$$

was used as a measure of the performance of the neural network. Here, P is the crystal size predicted by the neural network, and D is the actual measured diameter.

Feature Extraction

Wavelet analysis is becoming a common tool for analysing localised features in an image(Torrence and Compo, 1998). Specifically, for images, the localised support supplied by the wavelet basis functions provide an efficient compression algorithm e.g. for the storage of fingerprints. In our application, an efficient compression implies that the wavelet coefficients provide an efficient characterisation of the crystal sizes within the images.

However, there still needs to be a scheme to optimise the selection of the wavelet coefficients to reduce the dimensionality of the image (typically each image is 512×512 pixels) and hence the number of inputs to the neural network. Recognising that it is not necessary to retain the positional information of the different crystals, we have found that using the mean of either the coefficients in each of the 81 wavelet scale sizes or just the 9 diagonal scale sizes produces acceptable results.

A performance comparison for different wavelet families (Daubechies, Haar, Symlet and Coiflet) is tabulated in Table 1.

Table 1: Neural network performance with different wavelet bases.

Network Performance	***Daubechies***	***Haar***	***Symlet***	***Coiflet***
Mean Error (%)	10.96	13.62	12.13	11.65

Interestingly enough, although not surprisingly, the results using either the Daubechies, Haar, Symlet or Coiflet wavelets are similar. This would imply that although the mappings would be different, the different bases describe the different features differently, but all have basically the same information content. However, since the Daubechies wavelet exhibited the smallest mean error, it was used for the rest of the analysis.

Results

The results obtained for simulated crystals are shown in Figure 7 below. There is good linear correlation between the mean pixel size predicted by the neural network and the randomly generated crystal sizes.

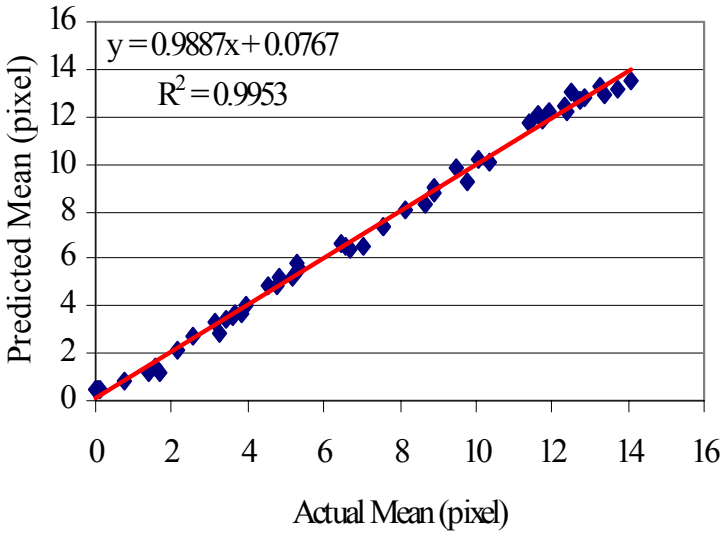

Figure 7: Performance of the neural network on unseen, noisy artificial images.

Figure 8 below shows the results using 144 pan images obtained from Tongaat-Hulett. Although originally 640×480 pixels in size, these images were first resized to 512×512 pixels as required by the wavelet algorithm. There is fairly good correlation between 60 µm and 230 µm with M = 9.0%.

It was also observed that the performance of the neural network was very sensitive to the choice of the training data. In particular, the MLP generalises well on a problem when it is trained on a well-selected data set that spans the range of features that will be present in the test set. Hence for good generalisation, it is important that:

a. There is a sufficiently large set of training data to avoid extrapolation.
b. The training set must be noise-free, i.e. not contain any bad (out of focus) images.
c. The training set must span the range of inputs that will be found in the unseen data set.

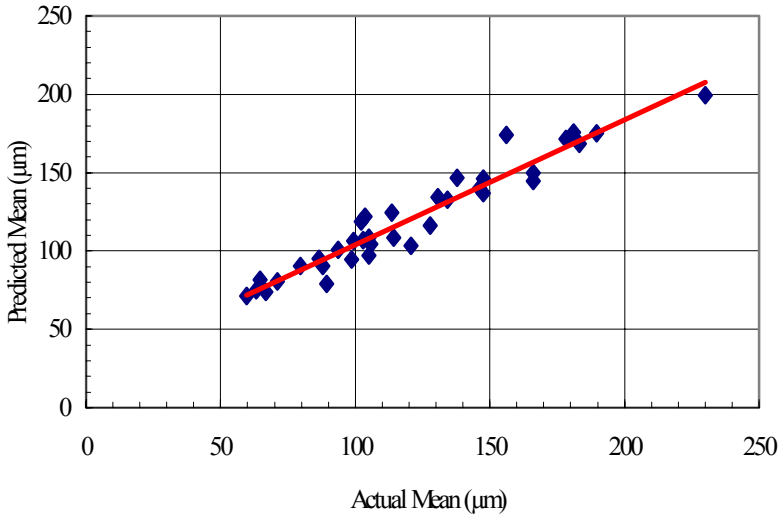

Figure 8: Performance of the neural network using the Tongaat- Hulett pan images.

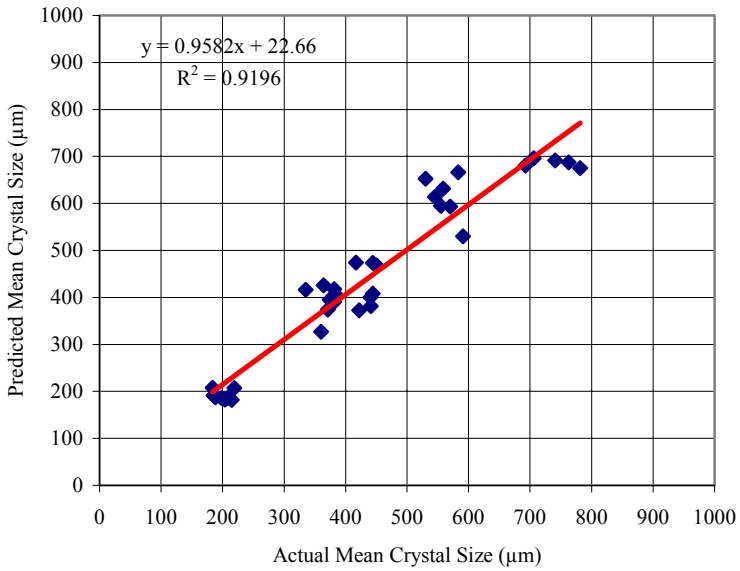

Figure 9: Performance of the neural network for images obtained from a laboratory crystaloscope immersed in a glycerine solution of sugar crystals.

Upon close examination of those images that were not well predicted, it was noticed that many of them suffered from poor illumination or were out of focus. For this reason it was decided to obtain another set of images using the crystaloscope under more controlled lighting conditions.

For this next test, five sieved sugar samples with nominal mean sizes of 100µm, 355µm, 500µm, 600µm and 850µm were prepared by the SMRI. About 25 such samples were taken from each of these samples and imaged using the crystaloscope. The mean crystal size in each image was measured manually using a Graphical User Interface (GUI) program.

Figure 9 shows the predicted output from the neural network versus the actual mean diameter, using the sums of the coefficients in each wavelet scale length as inputs. Here, M was 12.9%. There appears to be some systematic deviation for the 600µm and 850µm samples. A significant factor, which has not been taken into account, is the aspect ratio of the crystals. Whilst the wavelet coefficients should describe this information, crystals with different aspect ratios are being described by a single parameter *D*. To investigate whether this effect could be the reason for the systematic departure from the predicted crystal sizes, it will be necessary to include the crystal aspect ratio as an additional desired input to the neural network.

Discussion and Conclusion

We have demonstrated that it is possible to obtain an online measurement of the mean crystal size distribution by automatically analysing images captured from a black and white CCD-camera, viewing crystals splashed onto a port window of a crystallisation pan or from a crystaloscope immersed in a sugar solution. An optimised selection of Daubechies wavelet coefficients is used as a set of inputs to an MLP artificial neural network. The neural network is initially trained using the manually measured crystal diameters. On a randomly chosen set of images, the neural network is able to predict the average of the crystal size distribution with a mean % error, M, of approximately 10%. We have identified the importance of the need to eliminate 'bad' images from the training data set.

Although the mean crystal size is the extracted feature in this current paper, the same experimental arrangement could be used for the online measurement of other features of the crystal population such as adequate seeding, the presence of two-size distributions, crystal aspect ratio, etc. Future work will involve setting up a prototype using images obtained directly from a crystaloscope attached to a pan.

Acknowledgements

We gratefully acknowledge the financial support of the South African National Research Foundation (NRF).

We would like to thank Tongaat-Hulett Sugar Limited, particularly their Messrs Dave Love and Dennis Walthew, for allowing us to use the pan images. We are also indebted to Dr Raoul Lionnet of the Sugar Milling Research Institute for supplying us with the crystaloscopes and pilot pan sugar samples, and for supporting this project.

REFERENCES

1 Moolman, DW, Aldrich, C, Schmitz, G and van de Venter, J. (1996). The interrelationship between froth characteristics and industrial floatation performance. *Minerals Engineering 9*: 837-854.

2 Prasad, M and Singh, K (1999). Electrical conductivity of sugar crystal as a measurement of its quality. *Taiwan Sugar* V46: 19-22

3 Dalziel,SM, Tan, SY, White, ET and Broadfoot, R (1999). An analysis system for crystal sizing. *Proc. 1999 Conference of the Australian Soc. Sugar Cane Technologists*, Townsville, Queensland, Australia, 27-30 April

4 Miller, KF and Beath AC (2000). The measurement of raw sugar crystal size by sieving and by laser diffraction. *22nd Proc. Australian Soc. Sugar Cane Technologists*

5 Jones, OD, White, ET and Butler, BK (2000). Estimating crystal growth rates using computed tomography. *Inverse Problems* V16: 1477-1485

6 Palenzuela, ESG and Cruz, PIV (1996). Techniques for classifying sugar crystallization images based on spectral analysis and the use of neural networks. *Proc. IWISPO '96 Third International workshop on Image and Signal Processing - Advances in Computational Intelligence*: 641-645

7 Peacock, SD (1998). An introduction to neural networks and their application in the sugar industry. *Proc S. Afr. Sug Technol Ass*.: 184-191

8 Principe, JC, Euliano, NR and Lefebvre, WC (2000). *Neural and Adaptive Systems: Fundamentals Through Simulations.* John Wiley and Sons, ISBN: 0471351679,

9 Daubechies, I (1992). Ten Lectures on Wavelets. *Society for Industrial and Applied Mathematics*, 357pp.

10 Torrence, C and Compo, G (1998). A practical Guide to wavelet analysis. *Bulletin of the American Meteorological Society*, 79: 61-78